Soft Matter

www.rsc.org/softmatter

Volume 9 | Number 15 | 21 April 2013 | Pages 3887–4114

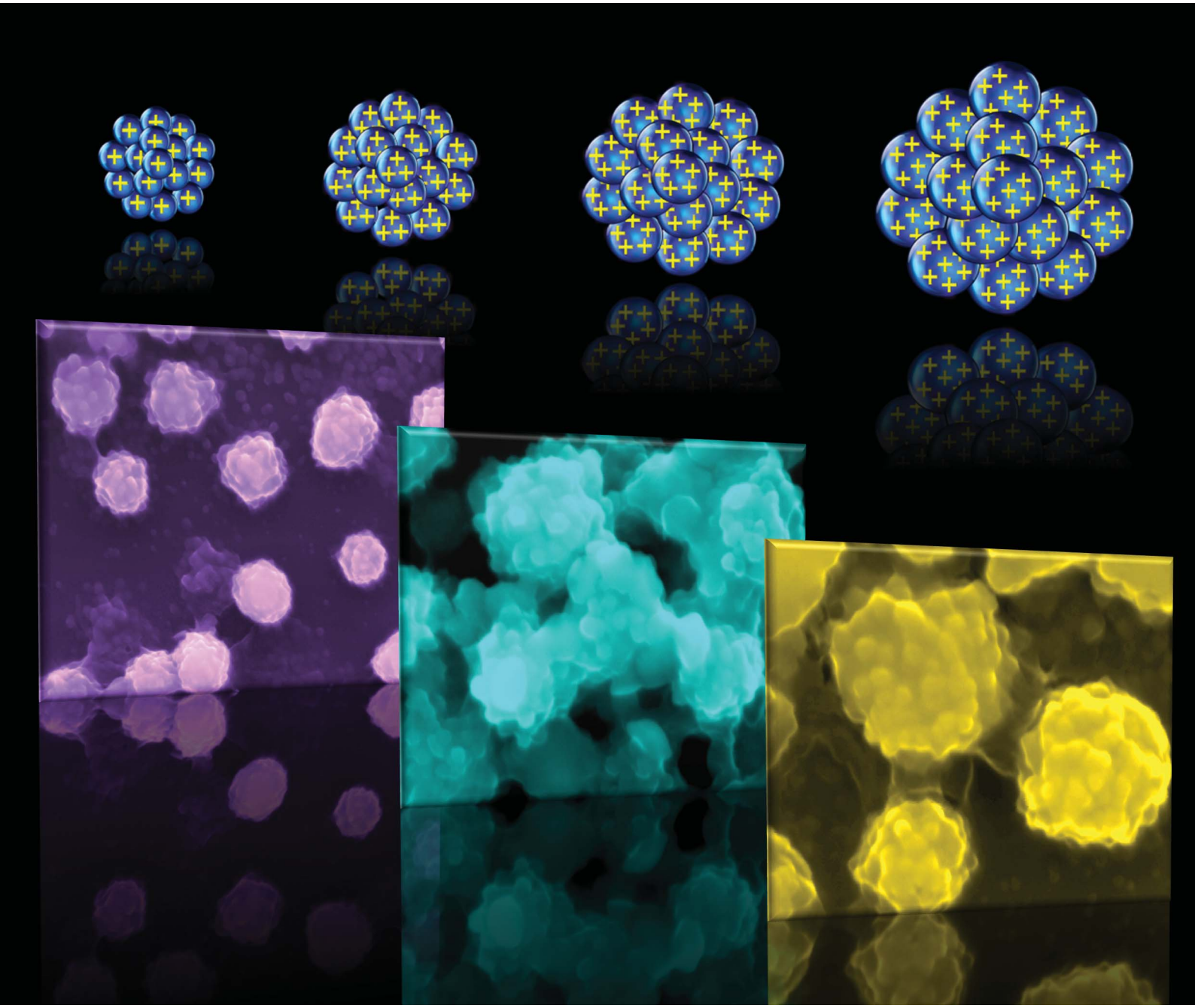

ISSN 1744-683X

RSC Publishing

PAPER

Brian R. Saunders *et al.*

Poly(vinylamine) microgels: pH-responsive particles with high primary amine contents

1744-683X(2013)9:15;1-6

Soft Matter

RSC Publishing

PAPER

View Article Online
View Journal | View Issue

Cite this: *Soft Matter*, 2013, **9**, 3920

Poly(vinylamine) microgels: pH-responsive particles with high primary amine contents†

Sineenat Thaiboonrod,[a] Cory Berkland,[b] Amir H. Milani,[a] Rein Ulijn[c] and Brian R. Saunders*[a]

pH-responsive microgels are crosslinked polymer colloid particles that swell when the pH approaches the pK_a of the polybase or polyacid chains. Poly(vinylamine) (PVAM) has the highest primary amine content of all amine-containing polymers. Despite much effort the preparation of colloidally stable PVAM microgels is still elusive. Here, we introduce a simple and scalable, two-step method for preparation of pH-responsive PVAM microgels. First, non-aqueous dispersion (NAD) polymerization was used to prepare new monodisperse water-swellable poly(*N*-vinylformamide-*co*-2-(*N*-vinylformamido)ethyl ether microgels (PNVF-*x*NVEE). Here, *x* is the mol% of the alkali-stable crosslinker (NVEE) used. Alkali-hydrolysis of the PNVF-*x*NVEE microgels in water gave colloidally stable poly(vinylamine-*co*-bis(ethyl vinylamine)ether) (PVAM-*x*BEVAME) microgel dispersions. SEM images showed that both the PNVF-9NVEE and PVAM-9BEVAME microgel particles had cluster-like morphologies. The PVAM-*x*BEVAME particles were positively charged at pH values less than 12. The hydrodynamic diameters and electrophoretic mobilities increased strongly as the pH decreased. In order to demonstrate that primary amines could be used as chemical handles for conjugation, pyrene carboxylic acid was coupled using *N*-(3-dimethylaminopropyl)-*N*′-ethylcarbodiimide (EDC) chemistry and its presence confirmed by fluorescence microscopy. Because this new family of colloidally stable microgels has very high primary amine contents and was prepared by a scalable synthetic method there should be potential applications in a wide range of areas from surface coatings and new hybrid particles to delivery.

Received 27th November 2012
Accepted 7th January 2013

DOI: 10.1039/c3sm27728c

www.rsc.org/softmatter

Introduction

Microgels are crosslinked polymer colloid particles that swell in a good solvent.[1–4] pH-responsive microgels swell when the pH approaches the pK_a of the constituent polybase or polyacid chains.[5] They have potential application in the areas of rheological modifiers, surface coatings,[6] photonic materials,[7] drug delivery[8] and regenerative medicine.[9] The overwhelming majority of research conducted on pH-responsive microgels has involved anionic, alkali-swellable, microgels containing carboxylic acid groups.[10–14] Acid-swellable microgels[15–22] and gel bead particles[23] containing primary amines are versatile systems for functionalization. Unfortunately, a method to prepare *colloidally stable* dispersions of microgels containing *high* primary amine contents has not been reported. Acid-swellable microgels based on secondary and tertiary amines have been well studied,[24,25] but they have limited potential for functionalization. Poly(vinylamine) (PVAM) is a very attractive design target for microgels containing primary amines because it contains the highest nitrogen content of all polycations[26] and has a very wide-range of functionalization reactions.[27] Unfortunately, the synthesis of dispersions of colloidally stable PVAM-rich microgels or, indeed, any other high content primary amine microgel has remained elusive. PVAM cannot be synthesized from vinylamine.[27] PVAM is commonly introduced post-polymerisation, *e.g.* by alkali-hydrolysis of the corresponding poly(*N*-vinylformamide) (PNVF) material to reveal the primary amine groups.[27,28] The harsh hydrolysis conditions required has obstructed attempts to prepare colloidally stable microgel dispersions with high primary amine contents. PVAM microgels are an important omission from the literature that has potential to provide a plethora of new functionalized microgels and microgel-based materials and hybrids. The motivation for this study was the need to establish a method for preparing colloidally stable pH-responsive PVAM microgel dispersions. Here, we introduce a new, scalable, two-step method to synthesize PVAM microgels and investigate the properties of the new microgels.

Our previous work involving poly(*N*-vinylformamide-*co*-glycidyl methacrylate) microgel particles offered a route to microgels

[a]*Polymer Science Research Group, Materials Building, School of Materials, The University of Manchester, Grosvenor Street, Manchester, M1 7HS, UK. E-mail: Brian.Saunders@manchester.ac.uk*

[b]*Department of Chemical and Petroleum Engineering and Department of Pharmaceutical Chemistry, The University of Kansas, Lawrence, Kansas 66047, USA*

[c]*Department of Pure and Applied Chemistry/WestCHEM, University of Strathclyde, Cathedral Street, Glasgow G1 1XL, UK*

† Electronic supplementary information (ESI) available. See DOI: 10.1039/c3sm27728c

containing PVAM.[19] However, the particles severely fragmented during alkali-hydrolysis due to cleavage of the crosslinks. Crosslink degradation is a well known general obstacle that frustrates synthesis of colloidally stable PVAM microgels.[22] Based on a report from the Kansas laboratory[29] we hypothesised that improved chemical stability to alkali-hydrolysis could be achievable by synthesizing of NVF particles containing a crosslinking monomer that was structurally related to NVF. We selected 2-(*N*-vinylformamido)ethyl ether (NVEE)[29,30] (Scheme 1) because it was expected to have a similar reactivity ratio to NVF and also contained an alkali-stable ether linkage that is resistant to cleavage. An aim of this study was to demonstrate the feasibility of functionalizing primary amine groups of the PVAM microgels. We used *N*-(3-dimethylaminopropyl)-*N*′-ethylcarbodiimide (EDC) – assisted conjugation for this purpose because it is widely used for functionalization of polymers (and biomaterials) containing primary amines.[31]

PVAM readily adsorbs onto anionic surfaces[32,33] and has been prepared as composite nanoparticles.[34] Well-defined amphiphilic core–shell particles containing a PVAM shell have been reported.[35] Recently, PVAM hydrogel shells[36] and hydrogel capsules have been reported.[37] Shi *et al.* studied the preparation of silica/PNVF clusters[38] and also PVAM micro and nanogel capsules.[39] In contrast to those studies, the PVAM microgel particles introduced here are *not* hollow. Therefore, microgel particles contain a much higher total primary amine contents (and functionalization capacity) than capsules. Microgels have an inherently higher elastic modulus than capsules because they have a higher number of elastically effective chains per particle. Our two-step synthetic method used to prepare colloidally stable pH-responsive PVAM microgel dispersions is depicted in Scheme 1. We used non-aqueous dispersion polymerization (NAD) to prepare new PNVF-*x*NVEE microgels (*x* is the mol% of NVEE employed) which were then hydrolysed to give poly(vinylamine-*co*-bis(ethyl vinylamine)ether) (PVAM-*x*BEVAME) microgels.

A finding of this study (from SEM images) was that PVAM-9BEVAME microgels had a cluster-like morphology. Cluster particles or popcorn-shaped particles have been reported earlier.[40–42] Li and Stover reported popcorn-shaped particles[40] for poly(divinylbenzene) particles prepared by NAD. The mechanism of their formation was attributed to adsorption of primary particles by larger monomer-swollen particles that were prepared early in the polymerization. Here, we provide the first report of pH-responsive microgel particles with cluster-like morphologies to our knowledge.

The structure of this paper is as follows. We first study a series of new water-swellable PNVF-*x*NVEE microgels and then hydrolyse them to pH-responsive PVAM-*x*BEVAME microgels. The morphologies of the microgel particles were characterised using SEM. Their compositions were probed using FTIR and quantified using elemental analysis. The pH-responsive properties of the PVAM-*x*BEVAME particles were measured using hydrodynamic diameter and electrophoretic mobility measurements. Finally, the ability to use the primary amine groups within the microgels for functionalization is

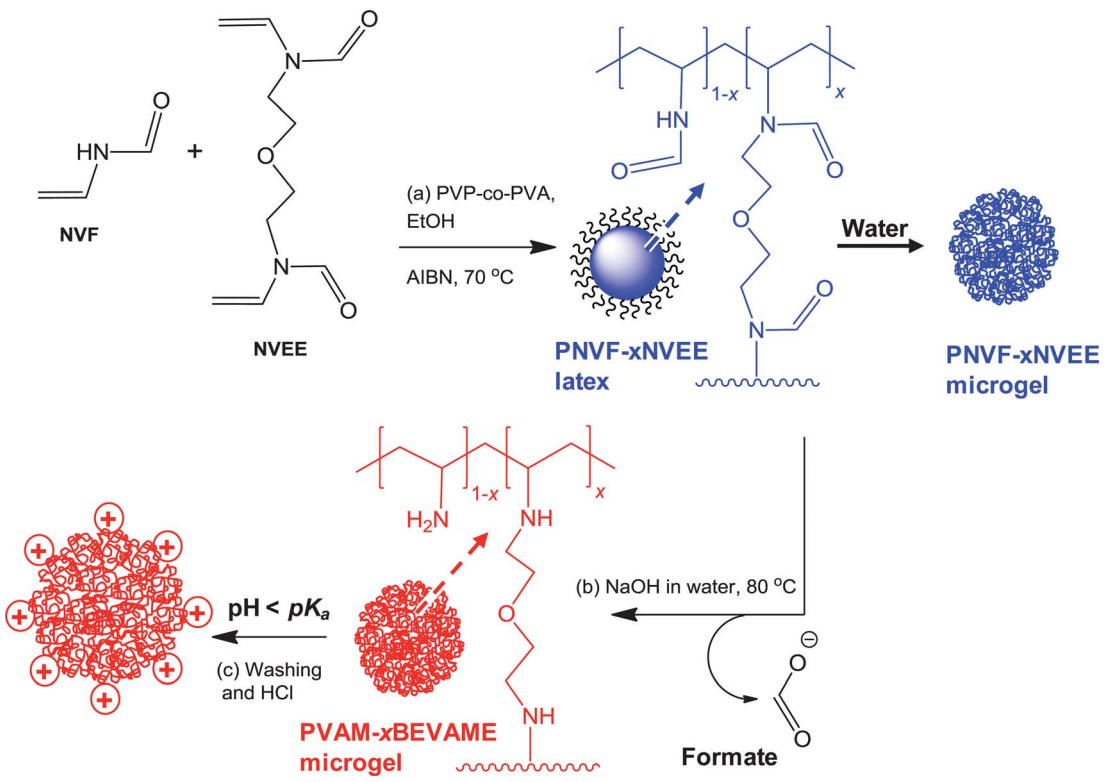

Scheme 1 Two-step synthesis of PVAM microgels. PNVF-*x*NVEE microgels were first prepared by non-aqueous dispersion polymerisation and then hydrolysed to PVAM-*x*BEVAME microgels. See text for abbreviations.

demonstrated. The new two-step method to synthesize PVAM microgels (Scheme 1) introduced here is scalable. The pH-responsive PVAM microgels introduced here should open up a wide range of potential applications from advanced surface coatings, hybrid particles,[43] rheological modifiers and delivery.

Experimental section

Materials

NVF (98%), azoisobutyronitrile (AIBN, 98%), potassium-*tert*-butoxide (95%), bis(2-bromoethyl)ether (BBE, 95%), dicyclohexyl-18-crown-6 (98%), anhydrous THF (99.9%), 1-pyrene carboxylic acid (PyC, 97%), fluorescein 5(6)-isothiocyanate (FITC, >90%) and ethanol (99.9%) were purchased from Aldrich and used as received. EDC (97%), *N*-Hydroxysuccinimde (NHS, 98%), cetyltrimethylammonium bromide (CTAB, 98%) and poly(1-vinylpyrrolidone-*co*-vinyl acetate) (PVP-*co*-PVA) were purchased from Aldrich and used as received. PVP-*co*-PVA had a weight-average molecular weight of 50 000 g mol^{-1} and a VA content of 43 mol%. The linear PVAM used here was prepared earlier by alkali-hydrolysis of PNVF particles and is described elsewhere.[19] High purity water that was distilled and deionised was used.

Crosslinking monomer synthesis

NVEE was synthesized using a modification to a method reported earlier[29] (see Scheme S1†). A mixture of NVF (7.1 g, 100 mmol), potassium-*tert*-butoxide (12.0 g, 105 mmol) and dicyclohexyl-18-crown-6 (1.00 g, 2.65 mmol) in THF was stirred vigorously and cooled to 0 °C. BBE (9.30 g, 40 mmol) was added dropwise to the mixture. The mixture was allowed to warm to room temperature and stirred for another 72 h. KBr was removed by filtration and the reaction mixture concentrated using rotary evaporation and diluted with water (100 mL). The product was extracted using chloroform washing and the extracts were combined and washed with brine and then dried over anhydrous sodium sulfate. NVEE was recovered from the chloroform solution as a liquid (5.69 g, 53% yield). The compositional purity of NVEE was confirmed by elemental analysis, ^{1}H NMR and FTIR spectroscopy (ESI, Fig. S1 and S2†). Based on ^{1}H NMR spectroscopy data (Fig. S1†) NVEE was a mixture of *trans* and *cis* isomers in the ratio of 1 : 2.

PNVF latex preparation

PNVF particles were prepared by NAD in latex form, *i.e.*, as non-swollen particles dispersed in ethanol. NVF (6 g, 85.5 mmol), AIBN (0.240 g, 1.45 mmol) and PVP-*co*-PVA (1.8 g) were added to ethanol (68 g) in a 4-neck round bottomed flask equipped with an overhead stirrer, nitrogen supply and a reflux condenser. The solution was purged using nitrogen and heated to 70 °C whilst being stirred vigorously. The polymerization time was 1 h. After cooling, the dispersion was purified by three centrifugation/redispersion cycles.

PNVF-*x*NVEE microgel synthesis

PNVF-*x*NVEE microgels were prepared in latex form (*i.e.*, as collapsed particles) using NAD using the procedure described above for PNVF. The value for x represents the mol% of NVEE used during preparation with respect to monomer. NVF (6 g, 85.5 mmol), AIBN (0.240 g, 1.45 mmol), PVP-*co*-PVA (1.8 g) and the appropriate mass of NVEE were added to ethanol (68 g) and the solution purged using nitrogen. The NVEE masses used were 0.845 g (3.91 mmol), 1.79 g (8.28 mmol) and 2.68 g (12.4 mmol), respectively, for PNVE-*x*NVEE where $x = 4$, 9 and 13. After cooling, the dispersion was purified by centrifugation using ethanol three times. The yield of recovered PNVF-9NVEE particles was 4.2 g.

PVAM-*x*BEVAME microgel synthesis

Alkali-hydrolysis was used to convert NVF and NVEE into, respectively, VAM and BEVAME (see Scheme 1). PNVF-*x*NVEE particles (1 g) were redispersed in aqueous NaOH solution (1 M) and heated, with stirring, at 80 °C under a nitrogen atmosphere for 16 h. For PNVF-*x*NVEE ($x = 9$ and 13) the hydrolysed dispersions were purified using repeated centrifugation and redispersion in water. In the case of PNVF-4NVEE the hydrolysis product was extensively dialysed against water. The yield of recovered PVAM-9BEVAME particles after purification by centrifugation was 0.33 g.

FITC-labelled PNVE-4NVEE and PVAM-4BEVAME microgel synthesis

FITC solution (20 μL, 2.6 mM) was added to the microgel dispersion (200 μL, 0.1 wt% dispersion). The dispersion was subjected to end-over-end mixing overnight.

Pyrene-labelled PVAM-9BEVAME microgel synthesis

The pH of a PVAM-9BEVAME dispersion (5 mL of 0.1 wt% dispersion in water) was adjusted to 6.8 using aqueous HCl (1 M). EDC (5.1 mg, 0.033 mmol) and NHS (3.9 mg, 0.034 mmol) were then added. The dispersion was stirred at room temperature before adding PyC (4.1 mg, 0.017 mmol) and the reaction was allowed to proceed for 18 h at room temperature. The product was purified by centrifugation and redispersion in PBS solution (0.15 M), NaCl solution (0.15 M) and then water. Physically absorbed PyC was removed by adding CTAB (0.1 M) to the dispersion and this was stirred overnight at room temperature before being repeatedly centrifuged and redispersed in water. A control dispersion was prepared and purified using the same method *without* added EDC and NHS.

Physical measurements

Elemental analysis (C, H, and N) was performed at the School of Chemistry, University of Manchester. Photon correlation spectroscopy (PCS) measurements were performed using a BI-9000 Brookhaven light scattering apparatus (Brookhaven Instrument Cooperation), fitted with a 20 mW HeNe laser and the detector was set at a scattering angle of 90°. (Measurements were also conducted at 30° and showed that the data were not angle dependent.) The particle volume swelling ratio (Q) was obtained using the hydrodynamic diameter measured by PCS at a given pH (d_h) and that measured for the particles in the collapsed

state ($d_{h(c)}$) using eqn (1). The value for ($d_{h(c)}$) was obtained using the particles dispersed in ethanol, which is a poor solvent for PNVF and PVAM.

$$Q = \left(\frac{d_h}{d_{h(c)}}\right)^3 \quad (1)$$

A Malvern Zetasizer was used to measure the electrophoretic mobilities of the particles in the presence of 0.001 M NaCl. SEM measurements were obtained using a Philips FEGSEM instrument. Samples were dried at room temperature. Optical microscopy was conducted with an Olympus BX41 microscope. Fluorescence microscopy was conducted on a Nikon Eclipse 50i microscope. Experiments involving PyC used a DAPI filter which allowed transmission of light at 475 nm. Experiments involving FITC used excitation and emission wavelengths of 480 and 535 nm, respectively. Attenuated total reflectance (ATR) Fourier transform infrared (FTIR) measurements were conducted using a Nicolet 5700 FTIR instrument.

Results and discussion

PNVF-*x*NVEE microgel particle swelling and morphology

PNVF-*x*NVEE latex dispersions ($x = 4$, 9 and 13) were prepared using NAD and had $d_{h(c)}$ values of 0.66 to 0.96 μm (Table 1). PNVF latex was also prepared for comparison. The dispersions were colloidally stable. Optical micrographs are shown in Fig. 1(a)–(d). For all of the dispersions examined in ethanol the particles appeared well defined (*e.g.*, Fig. 1(a)). When dispersed in water (Fig. 1(b)–(d)) they were more diffuse, which is an indication of swollen particles. This was confirmed by the values of Q for the particles dispersed in water (Table 1) which were much greater than 1.0. Additional evidence for particle swelling in water can be seen from the tubes shown in Fig. 1(a) and (b). PNVF-4NVEE particles were collected from ethanol as a white paste using centrifugation (Fig. 1(a)). When a small quantity of water was added a transparent physical gel rapidly formed (inset of Fig. 1(b)). PNVF-*x*NVEE is a new family of water-swellable microgels.

The extent of swelling for microgel particles usually decreases with increasing crosslinker concentration.[4] The data shown in Table 1 indicate a maximum Q of 7.0 for PNVF-9NVEE.

Table 1 Characterization data for PNVF-*x*NVEE dispersions

	d_h[a]/μm		Q[b]	D_{SEM}[c]/μm		
Code	Ethanol	Water	Water	Ethanol	Water	%N/%C[d]
PNVF	0.77	—	—	1.79 [6][e]	—	0.38
PNVF-4NVEE	0.96	1.38	3.0	1.26 [5][e]	—	0.36
PNVF-9NVEE	0.66	1.26	7.0	0.56 [10]	0.61 [10]	0.35
PNVF-13NVEE	0.80	1.11	2.7	0.75 [12]	0.70 [17]	0.34

[a] Hydrodynamic diameter. [b] Swelling ratio determined from the hydrodynamic diameters and eqn (1). [c] Number-average diameter measured from SEM. The coefficient of variation is shown in brackets. [d] Ratio of nitrogen and carbon contents determined by elemental analysis (see Table S1). [e] These values were affected by spreading (flattening) of the particles (see text).

The value for Q was only 3.0 for PNVF-4NVEE. The d_h value for the microgel was not as large as expected. When the shells of lightly crosslinked microgel particles fragment and detach from the cores the hydrodynamic diameter of microgels can decrease.[44] The lower Q than expected for PNVF-4NVEE combined with the inset of Fig. 1(b) (which confirms particle swelling) suggests that partial fragmentation of the shells occurred when PNVF-4NVEE particles were dispersed in water. Self-rupturing particles are interesting candidates for potential application in drug delivery.[45]

Fig. 2 shows SEM images for PNVF and the PNVF-*x*NVEE latex particles deposited from ethanol. Deformation (flattening) and coalescence of PNVF particles can be seen from Fig. 2(a) and (b). PNVF is a hydrophilic polymer.[30] Optical microscopy showed that within 5 min of deposition of the PNVF particles onto a microscope slide in air they had begun to spread and coalesce (see Fig. S3†). Particle spreading could be prevented if the deposited particles were stored over P_2O_5 which confirmed that spreading was due to absorption of water vapour. This effect, which is new for microgels, is a form of solvent vapour annealing.[46] SEM images showed that deposited PNVF-4NVEE particles (Fig. 2(d)–(f)) also coalesced when in contact with neighbouring particles (Fig. 2(d)). Well-separated particles (Fig. 2(e)) had the largest apparent number-average diameter as measured by SEM (D_{SEM}, Table 1). By contrast, deposited PNVF-9NVEE (Fig. 2(g)–(i)) and PNVF-13NVEE (Fig. 2(j)–(l)) particles that were closely packed did *not* coalesce. They also had smaller D_{SEM} values (Table 1), which is indicative of less spreading. The SEM data show that 9 mol% of NVEE was sufficient to give the shells of PNVF-*x*NVEE particles sufficiently high crosslink densities to resist inter-particle coalescence and film formation during drying.

Fig. 3 shows SEM images for PNVF-*x*NVEE particles deposited from water. The PNVF-4NVEE particles (Fig. 3(a)–(c)) spread considerably when deposited from water. Particle deformation due to spreading of microgel particles that were swollen prior to deposition has been frequently observed using SEM.[47,48] Here, many of the PNVF-4NVEE particles appeared to be absent (Fig. 3(a)) and circular voids were present. Those particles had flowed to a height lower than that of the surrounding material. The latter was debris from the fragmented PNVF-4NVEE shells. Dispersed PNVF-4NVEE microgel particle cores were observed in water by both optical microscopy (Fig. 1(b)) and fluorescence microscopy (Fig. 4(b)). The voids shown in Fig. 3(a) are an imprint of the swollen PNVF-4NVEE particle cores before the dispersion was completely dried. The average diameter of the circular voids was 1.8 μm (coefficient of variation of 7%), which is comparable to the d_h value for the microgel particles in water (1.38 μm, Table 1). Some flattened (fully spread) particles were evident – see the arrows in Fig. 3(a) and the expanded views (Fig. 3(b) and (c)).

More robust microgels were obtained using the higher x values. The SEM images for PNVF-9NVEE (Fig. 3(d)–(f)) and PNVF-13NVEE (Fig. 3(g–i)) particles deposited from water showed that they had low to moderate polydispersities. The microgels resisted coalescence when deposited from water (Fig. 3(d) and (g)) confirming that NVEE crosslinking was effective when x was 9 mol% or more. The higher magnification

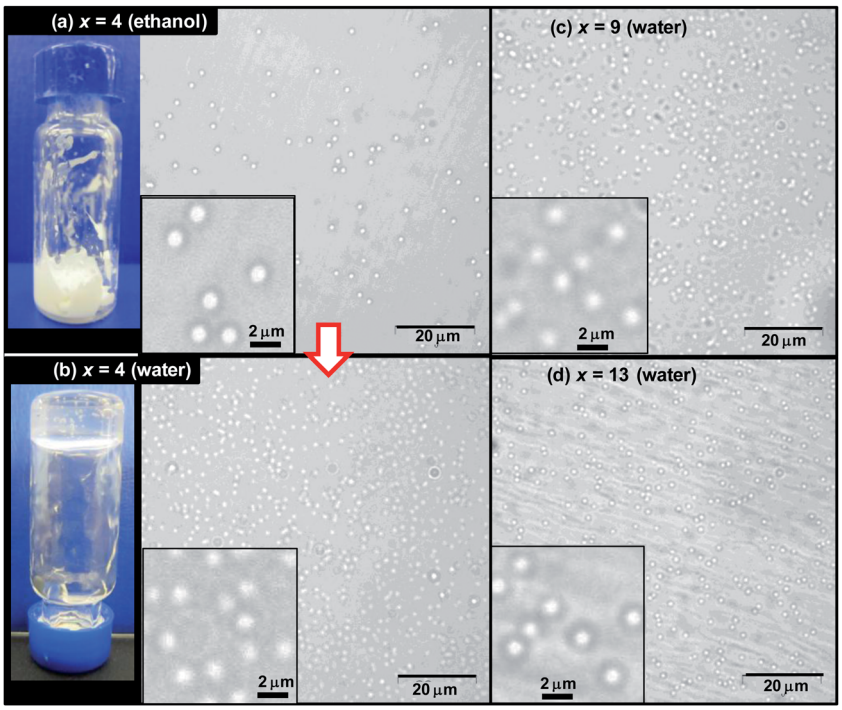

Fig. 1 Gel formation and optical micrographs for PNVF-*x*NVEE dispersions. (a) Shows PNVE-4NVEE latex particles dispersed in ethanol and centrifuged particles. (b) Shows PNVF-NVEE microgel particles dispersed in water and in concentrated form in water (see text). (c and d) Show PNVF-9NVEE and PNVF-13NVEE microgel particles dispersed in water.

image for PNVF-9NVEE (Fig. 3(f)) revealed that the particle surfaces had a cluster-like morphology. A representative higher magnification image for PNVF-13NVEE microgels is shown in Fig. 3(i). The outer region of the particles (indicated by the dotted circle) appeared to have flowed and deposited onto the substrate surrounding the core of the particles. This is consistent with a relatively lightly crosslinked PNVF-rich shell. A cluster-like morphology was not apparent for PNVF-13NVEE.

The widely accepted mechanisms for NAD are those proposed by Antl *et al.*[49] as well as Barrett and Thomas.[50] Accordingly, the mechanism for PNVF-*x*NVEE formation involves nucleation of primary polymer particles through aggregation of growing polymer chains that become insoluble in ethanol. The structures of NVEE and NVF (Scheme 1) show that NVEE is the more hydrophobic monomer. Therefore, we propose that NVEE-rich oligomers precipitated earlier during particle formation and the NVEE concentration was greatest in the core of the PNVF-*x*NVEE particles. After nucleation of the parent PNVF-*x*NVEE particles, colloidal stabilisation occurred due to adsorption of PVP-*co*-PVA. Aggregation ceased when the adsorbed surface concentration of PVP-*co*-PVA was sufficient to provide colloidal stability. Monomers were then adsorbed from the solution as particle growth continued at constant particle concentration.

PVAM-*x*BEVAME microgel morphologies, compositions and pH-responsive behaviours

PVAM-*x*BEVAME microgels were prepared by alkali-hydrolysis of PNVF-*x*NVEE (Scheme 1). The effective refractive index of the swollen PVAM-4BEVAME microgels was too close to that of water for the particles to be imaged using optical microscopy. Reaction of PVAM-4BEVAME microgel with FITC was used to visualize the particles using fluorescence microscopy (Fig. 4(a)). PNVF-4NVEE was used as a control system (Fig. 4(b)). The FITC-labelled PNVF-4NVEE particles appear sharp and distinct (Fig. 4(b)). The FITC-labelled PVAM-4VAME particles (Fig. 4(a)) appeared smaller and less bright. PCS data (Table 2) showed that the PVAM-4BEVAME microgels had the largest particle size. The reason they appeared smallest (Fig. 4(a)) in comparison to the other microgels is that the shells were highly swollen and could not be visualised by fluorescence microscopy. PCS measures the hydrodynamic diameter and is more sensitive to the peripheries of swollen particles. By contrast to PVAM-4BEVAME, optical images with microgel particles evident were readily obtained for PVAM-9BEVAME and PVAM-13BEVAME (Fig. 4(c) and (d)). These images imply less swelling occurred for those systems.

PCS data for the PVAM-*x*BEVAME microgels measured in water at pH = 7 are shown in Table 2 and the d_h values were in the range of 1.31–1.72 μm. These values are all larger than those for the respective non-hydrolysed PNVF-*x*NVEE microgels (Table 1). To probe the reversibility of particle swelling the PVAM-*x*BEVAME particles were redispersed in ethanol after having been first dispersed in water. In each case d_h decreased. However, the d_h values measured in ethanol (Table 2) were larger for both PVAM-9BEVAME and PVAM-13BEVAME compared to those for the respective PNVF-*x*NVEE particles measured in ethanol (Table 1). This shows partial irreversibility of particle swelling when the solvent was changed from a good to a poor

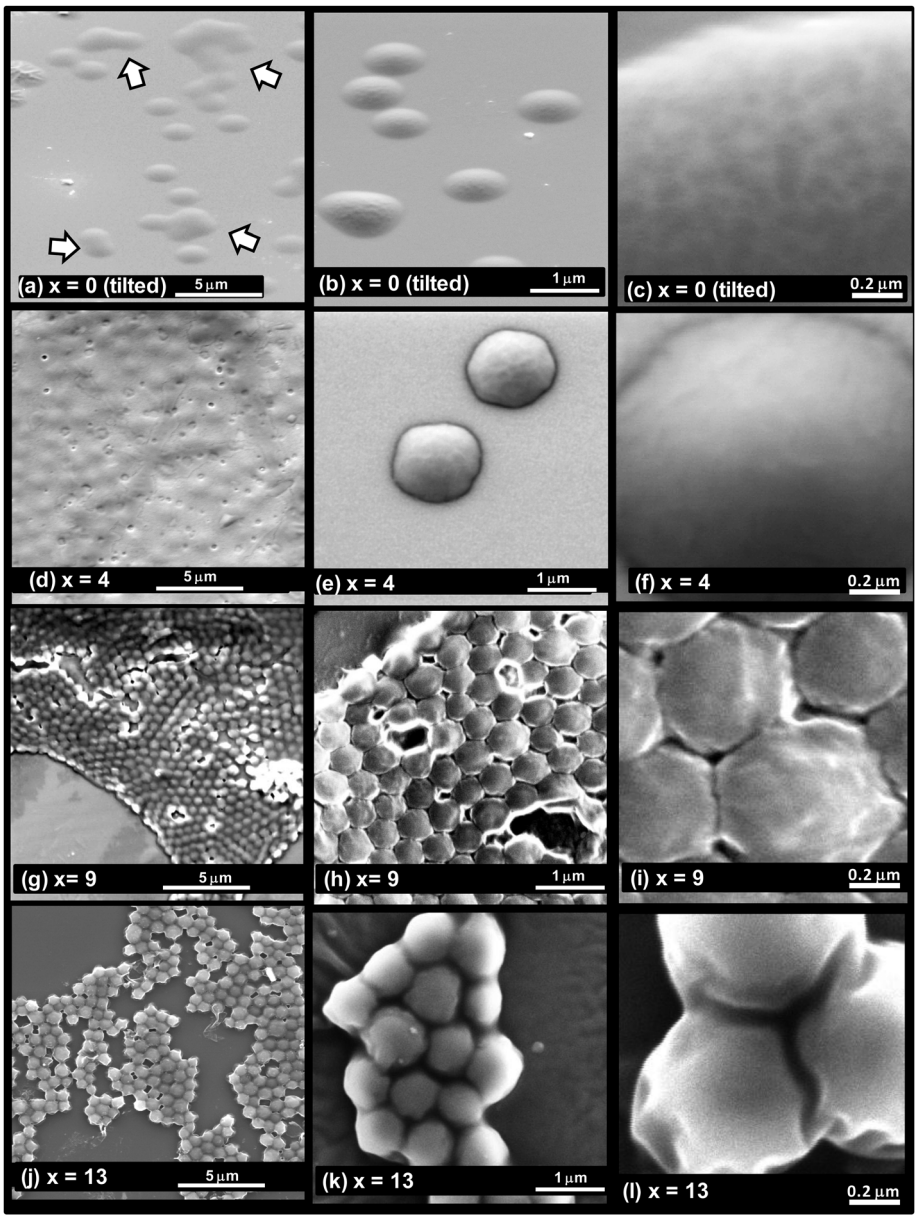

Fig. 2 PNVF and PNVF-*x*NVEE latex particles deposited from ethanol. The SEM images for PNVF particles (a–c) were obtained at an angle of 55° to the horizontal. The arrows in (a) show coalesced particles.

solvent. Complete hydrolysis of PNVF-*x*NVEE to PVAM-*x*BEVAME results in considerable mass loss because of the liberation of formate (Scheme 1). The mass loss was calculated to be in the range of 35–39 wt% for 100% hydrolysis depending on *x*. The intra-segment interactions that existed within the PNVF-*x*NVEE particles at the time of particle formation in ethanol will not be identical to those for the respective PVAM-*x*BEVAME particles when redispersed in ethanol. A significant proportion of the conformation changes required for reversible particle swelling must no longer have been possible after hydrolysis. By contrast, the value for d_h measured in ethanol for redispersed PVAM-4BEVAME particles (0.51 μm, Table 2) was much *smaller* than that for PNVF-4NVEE (0.96 μm, Table 1). This is further evidence of shell fragmentation for that system.

The calculation of *Q* values for PVAM-*x*BEVAME microgels was challenging because they were created in the swollen state, unlike conventional microgels. Furthermore, a mass loss due to hydrolysis and partial fragmentation was involved. Nominal *Q* values for PVAM-9BEVAME and PVAM-13BEVAME were estimated by using the d_h value for the respective parent PNVF-*x*NVEE latex in ethanol (Table 1) as the value for $d_{h(c)}$ (eqn (1)). These values should underestimate the true *Q* values because they did not take into account the mass loss due to hydrolysis described above. A different approach was used to estimate *Q* for PVAM-4BEVAME because that system underwent significant shell fragmentation. In that case the d_h value in ethanol for the as-made PNVF-4NVEE particles (Table 1) was not a meaningful value of $d_{h(c)}$ for the PVAM-4BEVAME microgel. For PVAM-4BEVAME the *Q* values

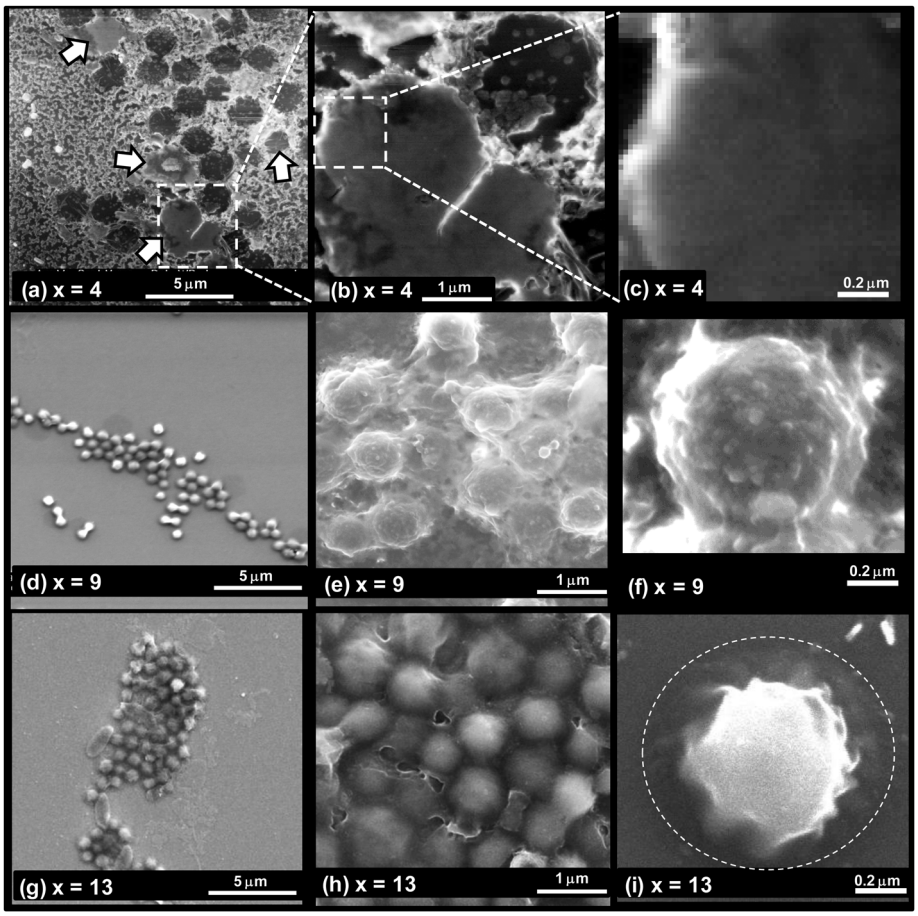

Fig. 3 PNVF-*x*NVEE microgel particles deposited from water. For the PNVF-4NVEE system (top row) nanoparticle debris from the shells surround regions where the microgel cores were present prior to SEM investigation. The arrows in (a) show flattened particles were still evident (see text). The dotted circle for (i) shows where the perimeter of the swollen particle had deposited prior to complete water evaporation.

were estimated using the d_h value for that microgel redispersed in ethanol (0.51 μm, Table 2). The Q values calculated in this way would also underestimate the true values because of the likelihood of partial irreversibility of microgel swelling in ethanol. The Q values at pH = 7 for the PVAM-*x*BEVAME microgels (Table 2) were all larger than those for the respective PNVF-*x*NVEE microgels (Table 1) due to ionised $PVAM^+$ groups. At pH = 7 each microgel contained at least 84 vol% water. The value for Q decreased with increasing x for the PVAM-*x*BEVAME microgels, as expected.

The PVAM-*x*BEVAME microgels were also investigated by SEM (Fig. 5). Major morphological changes occurred compared to the parent microgels (Fig. 3). The surface textures were more pronounced, presumably as a result of the mass loss that occurred due to hydrolysis discussed above. PVAM-4BEVAME showed a high population of narrowly dispersed particles (Fig. 5(a)). Higher magnification images showed a cluster-like morphology for those particles (Fig. 5(b) and (c)) as well as dispersed nanometer-sized particles (arrow in Fig. 5(b)). The former are the cores of the microgel particles. Some of the cluster-like particles had partially disintegrated (Fig. 5(c)). This is attributed to insufficient crosslinking. By contrast, the PVAM-9BEVAME particles ((Fig. 5(d)–(f)) showed remarkably well-developed, intact, cluster-like morphologies (Fig. 5(e) and (f)). A nodule type morphology has been previously reported for conventional poly(*N*-isopropylacrylamide) microgels.[51] However, the present surface morphology is much more pronounced.

For the highest x value used (PVAM-13BEVAME) the particle morphology was more uniform (Fig. 5(i)) and closer to that of the parent PNVF-13NVEE particles (Fig. 3(i)). This shows that the value for x controls the morphologies of the PVAM-*x*BEVAME particles and demonstrates tunability. We note that film formation of close packed PVAM-9BEVAME and PVAM-13BEVAME particles did not occur (Fig. 5(d) and (g)) which demonstrates that the crosslinking initially provided by NVEE survived hydrolysis for these systems. This confirms the stability of the ether linkage in NVEE.

Taken together, all the PCS, fluorescence microscopy and SEM data discussed above strongly support the view that PNVF-*x*NVEE and PVAM-*x*BEVAME particle shells had lower crosslinker concentrations than the cores. We interpret the morphological changes for the PVAM-*x*BEVAME particles (Fig. 5) with *decreasing* x in terms of *increasing* nanometer-scale fragmentation as a consequence of hydrolysis-triggered mass loss. As x decreased the consequence of the intra-particle crosslinker concentration decrease was most significant for the

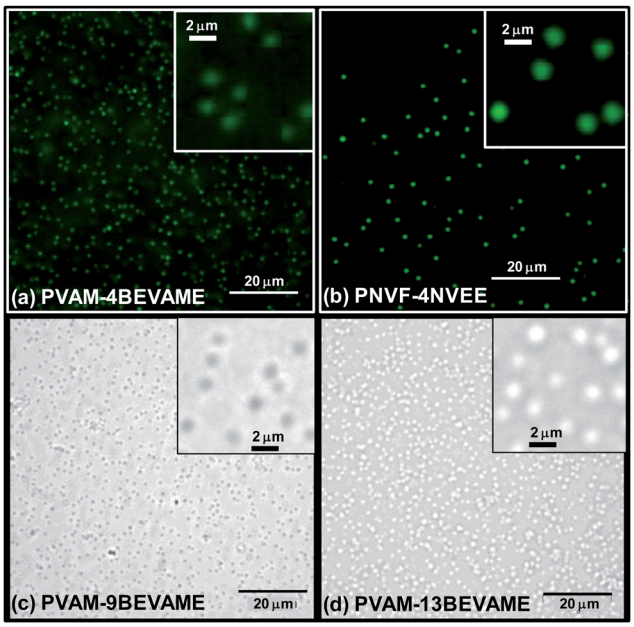

Fig. 4 PVAM-*x*BEVAME and PNVF-4NVEE microgel particle dispersed in water (a) and (b) show fluorescence micrographs of FITC-labelled particles. (c and d) Show optical micrographs. The pH was 7 in all cases. See images for sample identities.

particle shells. This caused fragmentation and release of increasing numbers of nanoparticles (see arrow in Fig. 5(b)). Some of this shell fragmentation may also have occurred prior to hydrolysis. Although we cannot be certain it is possible that the pronounced cluster morphology for PVAM-9BEVAME particles (Fig. 5(f)) occurred because the shell crosslinker concentration permitted localised nanometer-scale shell fragmentation. However, the extent of fragmentation was much less than that which occurred for PVAM-4BEVAME.

The compositional changes that accompanied hydrolysis of the PNVF-*x*NVEE microgels were probed using FTIR spectroscopy. The spectra for the PNVF-*x*NVEE microgels had a number of features in common with that of PNVF (see Fig. 6 and S4†). Those spectra all had bands that are due to[52] amide I (1650 cm^{-1}) and amide II (1540 cm^{-1}) and are consistent with spectra for PNVF reported earlier.[39] Alkali hydrolysis of the PNVF-*x*NVEE dispersions caused major changes in the spectra (see Fig. 6). The spectra for all of the PVAM-*x*BEVAME particles are very similar to that for PVAM. New bands appeared at 1590 cm^{-1} and in the vicinity of 3260 cm^{-1} due to RNH_2.[32,39,53] The FTIR spectra show that alkali-hydrolysis of the PNVF-*x*NVEE particles to PVAM-*x*BEVAME was successful.

The %N/%C ratio from elemental analysis data was used to quantify the extent of hydrolysis for PVAM-*x*BEVAME (see Table 2). The %N/%C values all *increased* (Table 2) compared to those of the parent microgels (Table 1), which is an important indicator of successful hydrolysis. The calculated percentage hydrolysis values range from 72% to 99% and agree with the trends established from the FTIR data (Fig. 6). Hydrolysis was effectively complete for PVAM-9BEVAME and PVAM-13BEVAME microgels. It is not clear why the conversion was lowest for PVAM-4BEVAME (72%). Nevertheless, the data show that very high proportions of primary amine groups were produced for each of the microgels and these dispersions were also colloidally stable. The mol% VAM in each microgel was calculated from the %N/%C values and values of up to 90% were determined (see Table 2). *The PVAM-xBEVAME microgels reported here contained the highest proportion of primary amine groups for any colloidally stable microgel dispersion reported to our knowledge*.

All of the PVAM-*x*BEVAME microgels exhibited strong pH-triggered swelling as judged by hydrodynamic diameter measurements (Fig. 7(a)). The microgels were swollen at pH = 12 which was partly due to the hydrophilic nature of PVAM. The pH-triggered increase in d_h upon decreasing the pH from 12 to 4 was greatest for PVAM-4BEVAME. For PVAM-9BEVAME and PVAM-13BEVAME the pH-triggered swelling was less strong, which is due to the higher concentration of crosslinking units present. In each case considerable pH-triggered swelling had occurred when the pH had decreased to 10, which is the pK_a of PVAM.[54] The trends established here for these pH-responsive microgels are comparable to those reported by Shi and Berkland for hollow PVAM capsules which were prepared by a template-and-etch route.[39] The swelling is best compared in terms of the nominal Q values and these data are shown in Fig. 7(b). The values used for $d_{h(c)}$ were the same as used in Table 2 and were discussed above. The data reported in Fig. 7(b) show the expected trend that Q decreased with increasing x across the whole pH range. This can also be seen from plots of d_h and Q data as a function of x (see Fig. S5(a) and (b)†). This is the first time this trend has been reported for PVAM microgels. *PVAM-xBEVAME microgels show*

Table 2 Characterization data for PVAM-*x*BEVAME microgels

	d_h[a]/μm						
Code	Water	Ethanol (redispersed)	Q[b]	D_{SEM}[c]/μm	%N/%C[d]	%Hyd.[e]	X_{VAM}/mol%[f]
PVAM	—	—	—	—	0.54[e]	83[g]	83[g]
PVAM-4BEVAME	1.72	0.51	38	0.84 [12]	0.48	72	69
PVAM-9BEVAME	1.31	1.04	7.8	0.50 [15]	0.50	99	90
PVAM-13BEVAME	1.46	1.10	6.1	0.69 [14]	0.47	96	84

[a] Hydrodynamic diameter measured in water (pH = 7) or when redispersed in ethanol. [b] Nominal volume swelling ratio at pH = 7 (see text). [c] Number-average diameter measured from SEM images. The coefficient of variation is shown in the brackets. [d] Ratio of nitrogen and carbon contents determined by elemental analysis. All elemental analysis data are shown in Table S1.† [e] % Hydrolysis calculated using: %Hyd. = 100 $[((7x + 3)/(x + 1)) - (1.1662/(\%N/\%C))]$. [f] mol% of VAM calculated from the product of %Hyd. and x. [g] From ref. 19.

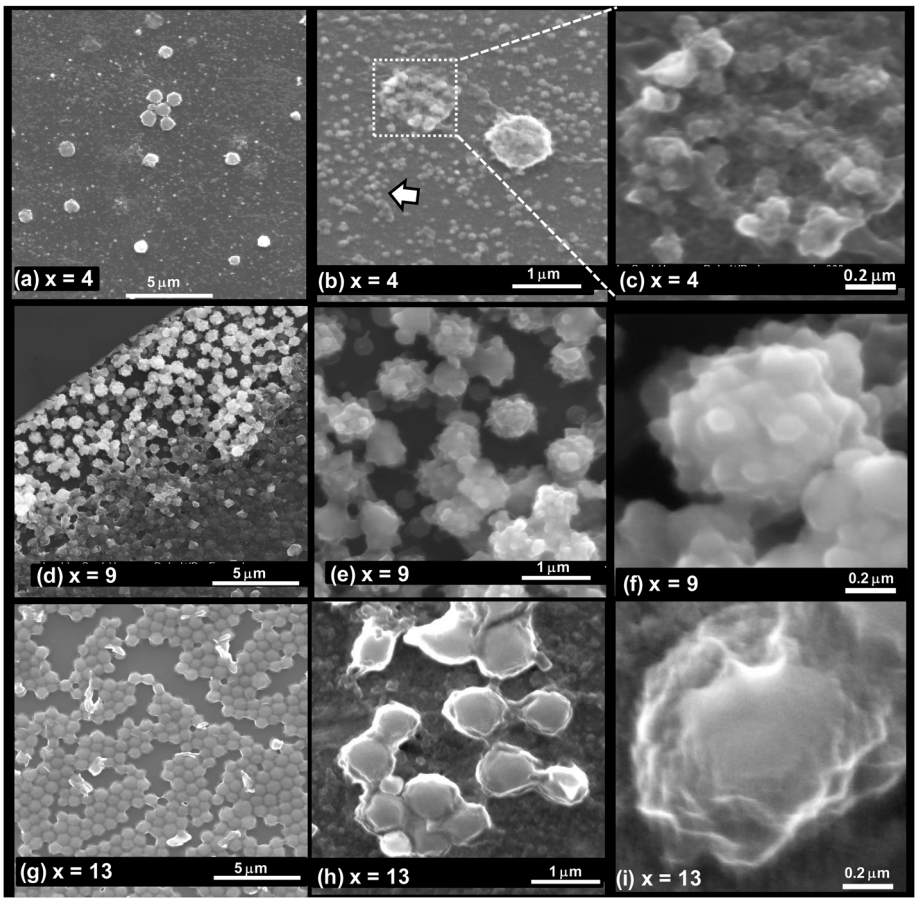

Fig. 5 PVAM-*x*BEVAME microgels deposited from water. The arrow in (b) identifies nanometer-sized particle fragments. The identities of the systems are given in the figures.

strong pH-triggered swelling when the pH decreases and the extent of swelling is tuneable using x.

The electrophoretic mobilities of the dispersions were measured as a function of pH (Fig. 7(b)). The mobilities were all positive and increased as the pH decreased for each of the PVAM-*x*BEVAME microgels. It is the increase in positive charge, and hence increased mobile ion concentration within the particles, that was responsible for the pH-triggered swelling shown in Fig. 7(a) and (b). Positive electrophoretic mobilities at all pH values of less than or equal to 10 is a further indication of successful hydrolysis for our PVAM-*x*BEVAME microgels because the pK_a of PVAM is[54] 10. The data from Fig. 7 were plotted as a function of *x* (see Fig. S5(c)†). The electrophoretic mobilities at pH = 4 and 7 increased substantially with decreasing *x*. At pH less than or equal to about 7 the positive charge density at the periphery of the particles is highest for the microgels prepared using the *least* crosslinker concentrations. PVAM-4BEVAME cores must have had a periphery composed of dangling, PVAM chains. By contrast, the PVAM-13BEVAME particles swelled the least, and showed the smallest electrophoretic mobility increase, with decreasing pH (Fig. 7(a)). These trends are indicative of a more highly crosslinked shell. A high crosslink density may oppose protonation as confined polycationic chains are known to have decreased apparent pK_a[55] values.

Demonstration of PVAM-9BEVAME microgel functionalization using primary amines

To demonstrate the potential for the primary amines of the microgels to act as chemical handles we covalently linked PyC onto the PVAM-9BEVAME microgels using EDC chemistry. As a control experiment PyC was mixed with the microgel without

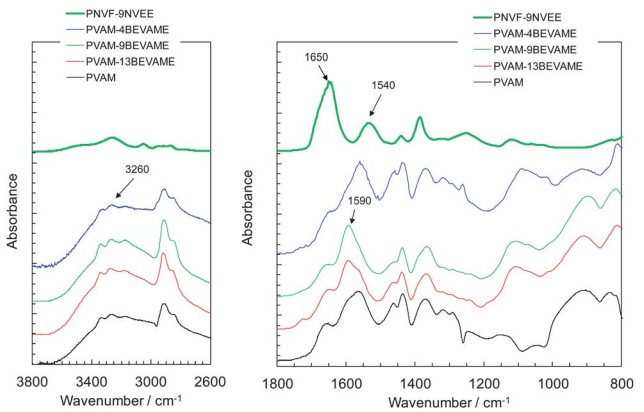

Fig. 6 FTIR spectra of PNVF-9NVEE and PVAM-*x*BEVAME microgels. The spectrum for linear PVAM is shown for comparison. The spectra for PNVF and the other PNVF-*x*NVEE microgels are shown in Fig. S4.†

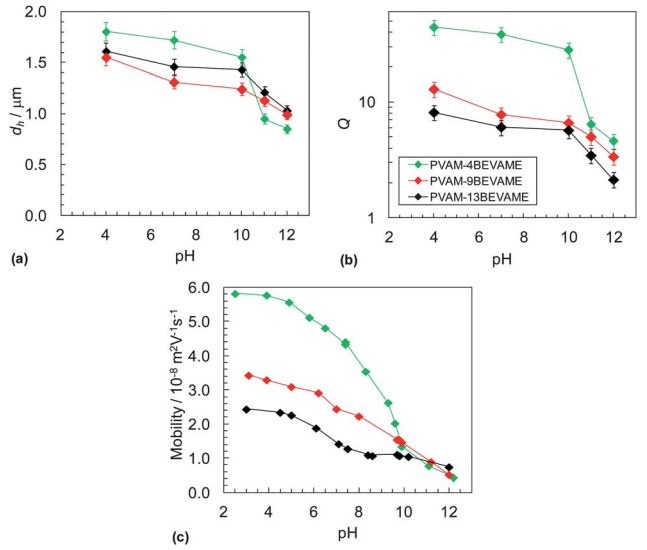

Fig. 7 pH-responsive behaviours of PVAM-*x*BEVAME microgels. (a and b) Show the variation of the hydrodynamic diameters and *Q* values, respectively with pH. (c) Shows the variation of the electrophoretic mobility with pH. The lines are guides for the eye. The error bars for the electrophoretic mobilities are smaller than the data points. The legend applies to both graphs.

EDC and NHS. To remove PyC the microgels were washed extensively with aqueous NaCl (0.15 M) solution, CTAB solution and then water. The fluorescence and optical micrographs obtained after this procedure are shown in Fig. 8. The fluorescently labelled particles were clearly observed for the particles where EDC/NHS was used (Fig. 8(a)). However, no particles were imaged for the control sample (no EDC/NHS, (Fig. 8(c)). The optical micrographs confirmed the presence of particles in each case (Fig. 8(b) and (d)). *These data demonstrate successful functionalization of PVAM-9BEVAME microgels using primary amine groups.*

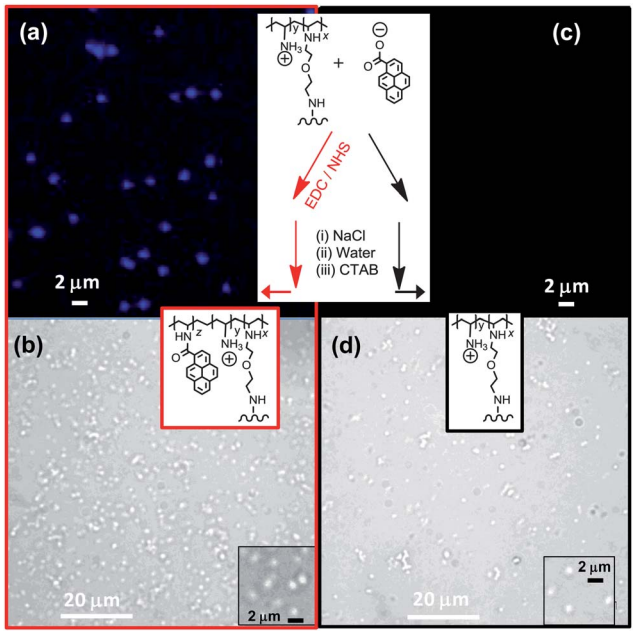

Fig. 8 Pyrene-labelling of PVAM-9BEVAME microgels. PVAM-9BEVAME microgels were mixed with PyC in the presence (a and b) or absence (c and d) of EDC/NHS and then extensively washed (see text). Fluorescence (a and c) and optical microscopy (b and d) images for the washed dispersions are shown.

Conclusions

This study has established two new families of microgels; PNVF-*x*NVEE and PVAM-*x*BEVAME. PVAME-*x*BEVMAE are a new family of colloidally stable pH-responsive microgels that contain very high primary amine contents and were prepared using a scalable two-step method. All of the data obtained in this study suggest that the cores of the PVAM-*x*BEVAME microgel particles are more highly crosslinked than the shells. It was found that the shells of the PNVF-4NVEE microgels fragmented when the value for *x* was 4 mol%. A value for *x* of 9 mol% (or higher) provided microgels PNVF-*x*NVEE microgels that were not susceptible to major inter-particle coalescence or fragmentation when hydrolysed. The PVAM-4BEVAME and PVAM-9BEVAME particles had a cluster-like morphology. This potentially useful particle morphology is controlled by *x* and is tuneable. Particles with built-in surface texture are of considerable academic interest.[40–42,56] The PVAM-*x*BEVAME microgels were strongly pH-responsive and their hydrodynamic diameters and electrophoretic mobilities increased substantially when the pH was decreased. The particles had hydrolysis extents of 72 to 99%. We demonstrated the chemical versatility of the new PVAM-9BEVAME microgels by using the primary amine groups as chemical handles to covalently link a RCOOH-functionalised dye. This study has provided a new method for preparing colloidally stable dispersions of high primary amine content microgels. PVAM is structurally related to polyethyleneimine (PEI) which has been widely used for DNA delivery.[57] Our new microgels should have potential application in a number of areas from advanced surface coatings, rheological modifiers, hybrid particles and delivery.

Acknowledgements

We would like to thank the Royal Thai government and the EPSRC for funding. Dr J. Gough and Prof. Peter Lovell are thanked for access to the fluorescence instrument and access to the PCS instrument.

References

1 A. Fernandez-Barbero, I. J. Suarez, B. Sierra-Martin, A. Fernandez-Nieves, F. J. de las Nieves, M. Marquez, J. Rubio-Retama and E. Lopez-Cabarcos, *Adv. Colloid Interface Sci.*, 2009, **147–148**, 88.
2 L. A. Lyon, Z. Meng, N. Singh, C. D. Sorrell and A. St. John, *Chem. Soc. Rev.*, 2009, **38**, 865.
3 R. Pelton, *Adv. Colloid Interface Sci.*, 2000, **85**, 1.
4 B. R. Saunders, N. Laajam, E. Daly, S. Teow, X. Hu and R. Stepto, *Adv. Colloid Interface Sci.*, 2009, **147–148**, 251.
5 J. McParlane, D. Dupin, J. M. Saunders, S. Lally, S. P. Armes and B. R. Saunders, *Soft Matter*, 2012, **8**, 6239.

6 P. Bradna, P. Stern, O. Quadrat and J. Snuparek, *Colloid Polym. Sci.*, 1995, **273**, 324.
7 L. A. Lyon, J. D. Debord, S. B. Debord, C. D. Jones, J. G. McGrath and M. J. Serpe, *J. Phys. Chem. B*, 2004, **108**, 19099.
8 J. Zhou, G. Wang, L. Zou, L. Tang, M. Marquez and Z. Hu, *Biomacromolecules*, 2008, **9**, 142.
9 A. H. Milani, A. J. Freemont, J. A. Hoyland, D. J. Adlam and B. R. Saunders, *Biomacromolecules*, 2012, **13**, 2793.
10 T. Hoare and R. Pelton, *Macromolecules*, 2007, **40**, 670.
11 M. Karg, Y. Lu, E. Carbo-Argibay, I. Pastoriza-Santos, J. Perez-Juste, L. M. Liz-Marzan and T. Hellweg, *Langmuir*, 2009, **25**, 3163.
12 J. Kleinen and W. Richtering, *J. Phys. Chem. B*, 2011, **115**, 3804.
13 R. Liu, A. H. Milani, T. J. Freemont and B. R. Saunders, *Soft Matter*, 2011, **7**, 4696.
14 C. D. Sorrell and L. A. Lyon, *J. Phys. Chem. B*, 2007, **111**, 4060.
15 A. Garcia, M. Marquez, T. Cai, R. Rosario, Z. Hu, D. Gust, M. Hayes, S. A. Vail and C.-D. Park, *Langmuir*, 2007, **23**, 224.
16 X. Hu, Z. Tong and L. A. Lyon, *Colloid Polym. Sci.*, 2011, **289**, 333.
17 Z. Hu and H. Gang, *Angew. Chem., Int. Ed.*, 2003, **42**, 4799.
18 D. Gan and L. A. Lyon, *Prog. Colloid Polym. Sci.*, 2006, **133**, 1.
19 S. Thaiboonrod, F. Cellesi, R. V. Ulijn and B. R. Saunders, *Langmuir*, 2012, **28**, 5227.
20 J. Xu and R. Pelton, *J. Colloid Interface Sci.*, 2004, **276**, 113.
21 J. Xu, A. B. Timmons and R. Pelton, *Colloid Polym. Sci.*, 2004, **282**, 256.
22 C. Miao, X. Chen and R. Pelton, *Ind. Eng. Chem. Res.*, 2007, **46**, 6486.
23 T. O. McDonald, H. Qu, B. R. Saunders and R. V. Ulijn, *Soft Matter*, 2009, **5**, 1728.
24 J. M. D. Heiji and F. E. Du Prez, *Polymer*, 2004, **45**, 6771.
25 D. Dupin, S. Fujii, S. P. Armes, P. Reeve and S. M. Baxter, *Langmuir*, 2006, **22**, 3381.
26 H. Ajiro, Y. Takemoto, T.-A. Asoh and M. Akashi, *Polymer*, 2009, **50**, 3503.
27 R. K. Pinschmidt, *J. Polym. Sci., Part A: Polym. Chem.*, 2010, **48**, 2257.
28 L. Gu, S. Zhu and A. N. Hrymak, *J. Appl. Polym. Sci.*, 2002, **86**, 3412.
29 Z. Mohammadi, A. Cole and C. Berkland, *J. Phys. Chem. C*, 2009, **113**, 762.
30 T. C. Suekama, V. Aziz, Z. Mohammadi, C. Berkland and S. H. Gehrke, *J. Polym. Sci., Part A: Polym. Chem.*, 2013, **51**, 435.
31 J. M. Klostranec and W. C. W. Chan, *Adv. Mater.*, 2006, **18**, 1953.
32 S. Seifert, F. Simon, G. Baumann, M. Hietschold, A. Seifert and A. Spange, *Langmuir*, 2011, **27**, 14279.
33 Q. Wen, A. M. Vincelli and R. Pelton, *J. Colloid Interface Sci.*, 2012, **369**, 223.
34 V. V. Annenkov, E. N. Danilovsteva, V. A. Pal'shin, V. O. Aseyev, A. K. Petrov, A. S. Kozlov, S. Patwardhan and C. C. Perry, *Biomacromolecules*, 2011, **12**, 1772.
35 W. Li and P. Li, *Macromol. Rapid Commun.*, 2007, **28**, 2267.
36 J.-H. Han, B.-M. Koo, J.-W. Kim and K.-D. Su, *Chem. Commun.*, 2008, 984.
37 J. Kim, H.-J. Lim, Y. K. Hwang, H. Woo, J. W. Kim and K. Char, *Langmuir*, 2012, **28**, 11899.
38 L. Shi, S. Khondee, T. Linz and C. Berkland, *Macromolecules*, 2008, **41**, 6546.
39 L. Shi and C. Berkland, *Macromolecules*, 2007, **40**, 4635.
40 K. Li and H. D. Stover, *J. Polym. Sci., Part A: Polym. Chem.*, 1993, **31**, 2473.
41 L.-M. Zhou, S. Shi, S.-I. Kuroda and H. Kubota, *Chem. Lett.*, 2007, **36**, 624.
42 K.-C. Lee, M. A. Winnik and T.-C. Jao, *J. Polym. Sci., Part A: Polym. Chem.*, 1994, **32**, 2333.
43 R. Contreras-Caceres, A. Sanchez-Iglesias, M. Karg, I. Pastoriza-Santos, J. Perez-Juste, J. Pacifico, T. Hellweg, A. Fernandez-Barbero and L. M. Liz-Marzan, *Adv. Mater.*, 2008, **20**, 1666.
44 S. Lally, F. Cellesi, T. Freemont and B. R. Saunders, *Colloid Polym. Sci.*, 2011, **289**, 647.
45 B. G. De Geest, C. Dejugnat, G. B. Sukhorukov, K. Braeckmans, S. C. De Smedt and J. Demeester, *Adv. Mater.*, 2005, **17**, 2357.
46 K. W. Gotrik, A. F. Hannon, J. G. Son, B. Keller, A. Alexander-Katz and C. A. Ross, *ACS Nano*, 2012, **6**, 8052.
47 K. Horigome and D. Suzuki, *Langmuir*, 2012, **28**, 12962.
48 B. R. Saunders and B. Vincent, *J. Chem. Soc., Faraday Trans.*, 1996, **92**, 3385.
49 L. Antl, J. W. Goodwin, R. D. Hill, R. H. Ottewill, S. M. Owens, S. Papworth and J. A. Waters, *Colloids Surf.*, 1986, **17**, 67.
50 K. E. J. Barrett and H. R. Thomas, Kinetics and mechanism of dispersion polymerization, in *Dispersion polymerization in organic media*, ed. K. E. J. Barrett, Wiley, London, 1975, ch. 4, p. 1975.
51 K. Kratz, T. Hellweg and W. Eimer, *Polymer*, 2001, **42**, 6631.
52 Y. Maeda, T. Higuchi and I. Ikeda, *Langmuir*, 2000, **16**, 7503.
53 R. C. Weast, M. J. Astle and W. H. Beyer, *CRC Handbook of Chemistry and Physics*, CRC, Boca Raton, 65 edn, 1985.
54 K. Samaru, H. Matsuoka and H. Yamaoka, *J. Phys. Chem.*, 1996, **100**, 9000.
55 J. Suh, H.-J. Paik and B. K. Hwang, *Bioorg. Chem.*, 1994, **22**, 318.
56 X. Liu, X. Jin and P. X. Ma, *Nat. Mater.*, 2011, **10**, 398.
57 J. A. Hubell, *Gene Ther.*, 2006, **13**, 1371.

